

Mechanisms of wettability control on two-phase immiscible displacement in microfluidic porous media

Nang Kang · Peibing Xu, Cong Luo, Xie, Shuang mei Zou
Chang University of Geosciences (Wuhan)

ACCEPTED MANUSCRIPT

Introduction

Displacement mechanisms for immiscible fluids in porous media are very important for a wide range of hydrological and geological systems, such as natural resource management [1, 2]. In hydrocarbon reservoirs, displacement efficiency remarkably influences oil production due to the gravity, viscous, and wettability forces [3-5]. In enhanced oil recovery (EOR), wettability is a major factor controlling flooding, foam, and surfactant displacement [6-8]. A water-oil interface is usually considered as amphiphilic for its large contact area with the solid surface [9]. The displacement of oil by water is controlled by the balance of the hydrophilic and the oleophilic forces [10]. Wettability has been given much attention in the porous media field, with considerable research work being successfully applied to various fields, such as fluid distribution in the porous or solid matrix.

When the porous medium surface is rough, the wettability that the fluid imparts media is generally the complementary between surface and surface [11-13], which is often characterized by two dimensionless parameters: Capillary number (Ca) and Wettability index (W_i). Both of them describe the relative forces in different fluids, which is represented as:

$$W_i = \frac{\sigma \cos \theta}{\mu v}$$

where, σ and μ are the surface tension and the viscosity of the displacing fluid respectively, θ is the contact angle between the oil and water, and v is the contact angle (capillary velocity).

In general, higher wettability means to be obtained by reducing the Wettability index (W_i) which may be defined as:

$$W_i = \frac{\sigma \cos \theta}{\mu v}$$

where σ is the fluid surface tension.

Lorenzini [14] considered the displacement mechanism in microfluidic media that depends on a Ca and W_i . He revealed that the displacement pattern can be divided into immiscible displacement (1) viscous fingering, (2) viscous fingering and (3) wettability fingering.


First, fluid displacement into porous or solid matrix can be considered as immiscible displacement, depending on the flow or wettability. During immiscible displacement, the flow is moving faster than the wettability that the solid matrix

Method and Materials

Experimental set-up


The microfluidic displacement experiment platform is shown in Fig. 1(a) and can be divided into the two-level flow-phase displacement experiment. The platform mainly consists of microfluidic mixing chamber, pressure sensor, imaging system and detection system. A high-resolution CMOS camera (Mikrotron H1280-202) is used to capture fluid flow in a micro-scale and single pressure sensor pump (the model is MP-1000-10) is used to achieve precise pressure control. Specific flow rates from 0.1 to 100 $\mu\text{L}/\text{min}$.

Fig. 1(a)



We conduct fluid displacement experiments in porous media (microfluidic) devices prepared with microchannels (channel diameter as shown in Fig. 1(b)). The structure in microfluidic device is similar to the porous medium. The media is 20 mm in length, 1.5 mm in width, with pore radius equal to 20 μm , porosity of 50%, permeability of 1.0 Darcy.

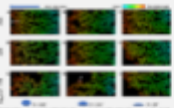
Fig. 1(b)




Results and Discussion

Oil-Water Two-Phase Porous-Media Displacement Experiment

Fig. 2 shows the advancing process of two-phase fluid into the porous media saturation and capillary number. Each figure shows the color between fluid-finger growth gradually transition to a uniform pattern, representing the wettability of the porous medium surface in the breakthrough. Blue represents the fluid distribution in the porous media, the wettability of the porous media (microfluidic media) and represents the relative wettability phase between the two fluids. In the two-phase displacement experiment, the viscosity ratio (λ) is chosen as 0.5, as shown in 1-5.



In the case of higher displacing rates ($\lambda = 0.5$), higher flow rates lead to more stable displacement patterns in all three wettability cases, media flow is more likely to become a regular pattern, and the capillary fingering phenomenon is more obvious. In the displacement experiment, instead of the immiscible displacement, the flow media is regular and stable, no experiments are observed in the three cases. The displacement pattern is the advancing fingering of the two-phase fluid, which may be the immiscible wettability ratio flow direction, which may be the permeability contrast appears in the main flow direction in Fig. 2(a). Under the condition of the same porosity, permeability and pore radius, the flow direction is the same.



OPEN ACCESS

[AUTHOR INFORMATION](#)
[REFERENCES](#)
[CONTACT AUTHOR](#)
[GET PAPER](#)

China University of Geosciences (Wuhan)



AGU FALL MEETING
New Orleans, LA & Online Everywhere
13–17 December 2021

Poster Gallery
brought to you by
WILEY

INTRODUCTION

Displacement mechanisms for two immiscible fluids in porous media are very important for groundwater hydrology and geological carbon sequestration as well as reservoir engineering[1]. It has been well recognized that reservoir wettability significantly influences oil production during primary, secondary, and tertiary recovery (enhanced oil recovery) stages[2-4]. Wettability is a major factor controlling the location, flow, and distribution of fluids in a reservoir[5]. Much of the research on multiphase flow in porous media has focused on the effect of fluid properties and flow conditions[6]. Much less emphasis has been given to the fluids' affinity to the porous media (i.e., wettability), even though wettability has a profound influence on fluid–fluid interactions in the presence of a solid surface.

When the gravitational effect can be neglected, the immiscible fluid flow in porous media is governed by the competition between viscous and capillary forces[7], which is often characterised by two dimensionless parameters: Capillary number (Ca) and Viscosity ratio (M)[8]. Here, Ca shows the effect of viscous to interfacial forces, which is represented as

$$Ca = \mu v / \sigma \cos \theta$$

where, v and μ are the velocity and viscosity of the displacing fluid respectively, σ is the interfacial tension between the oil and water, and θ is the contact angle that quantifies wettability.

In general, higher sweep efficiencies can be obtained by reducing the Viscosity ratio (M) which may be defined as

$$M = \mu_{\text{displacing phase}} / \mu_{\text{displaced phase}}$$

where μ is the fluid viscosity.

Lenormand[9] conducted displacement experiments in microfluidic cells that spanned a range of Ca and M. He concluded that three main displacement patterns are achieved during immiscible displacement: (1) viscous fingering, (2) capillary fingering and (3) stable displacement.

Fluid–fluid displacement in the presence of a solid surface can be characterized as either drainage or imbibition, depending on the system's wettability. Drainage refers to the regime where the invading fluid is less wetting to the solid surface than the defending fluid. Imbibition refers to the opposite case, where the invading fluid is more wetting to the solid surface than the defending fluid[10].

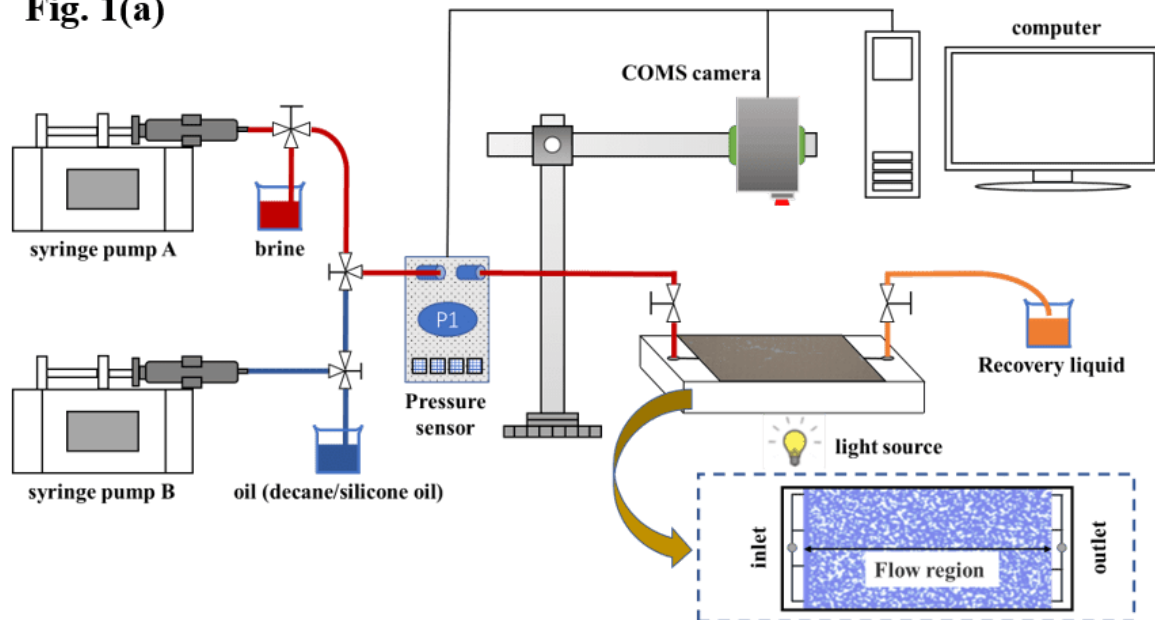
Here, brine-oil two phase microscopic displacement experiments under different injection conditions (velocity) in porous media with different wettability were carried out to study the influence mechanism of wettability and capillary number on brine-oil two phase flow characteristic, residual oil distributions and displacement efficiency.

METHODS AND MATERIALS

Experimental set-up

The micro-fluid visualization experiment platform as shown in **Fig.1(a)** was used to carry out the brine-oil two phase displacement experiment. The platform mainly consists of microfluidic model, pressure sensor, imaging system and flow control system. A high-resolution COMS camera (Manta G-1236C IRC) is used to capture fluid flow on a micron scale, and a high precision injection pump (Harvard Apparatus 70–3307) is used to achieve precise control of injection flow rates from 0.1 to 100 $\mu\text{l}/\text{min}$.

Fig. 1(a)



We conduct fluid-fluid displacement experiments in quasi-2D microfluidic flow models patterned with random pore channel network as shown in **Fig.1(b)**. The structure in microfluidic chips is created by an etching process. The model is 20 mm in length and 10 mm in width, with pore etched depth of 20 μm , pore volume of 7 μl , porosity of 0.52 and permeability of 1.6 Darcy.

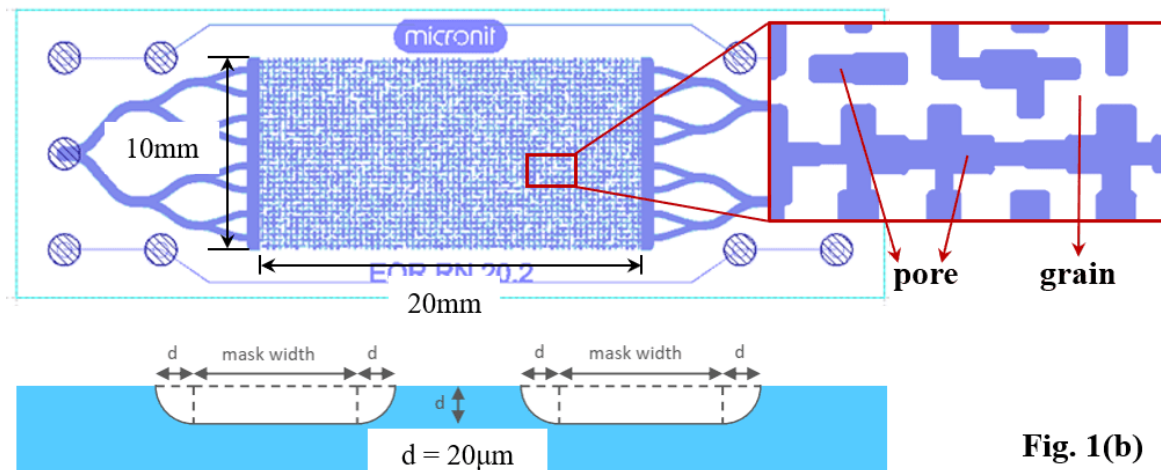
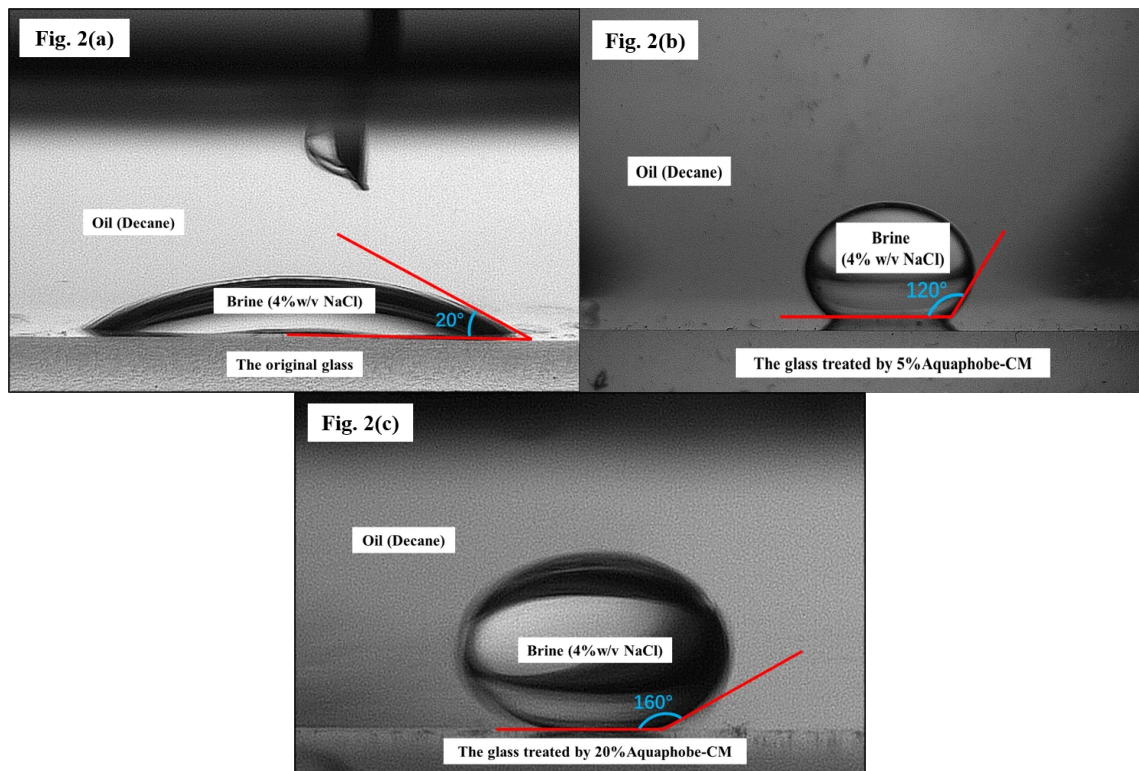


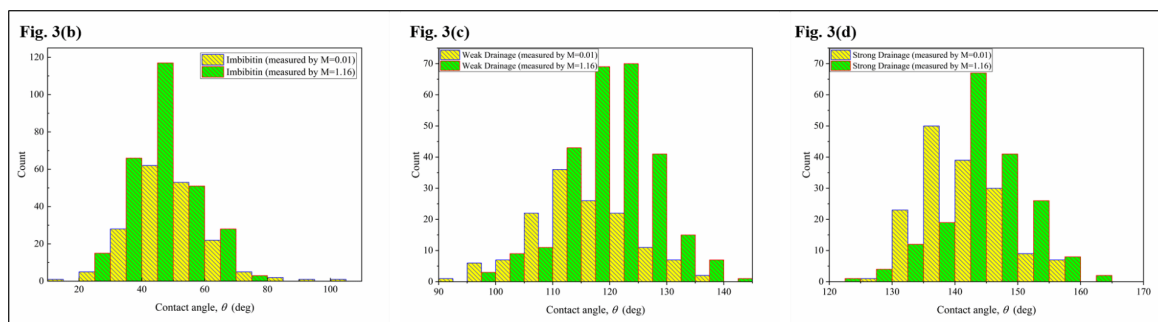
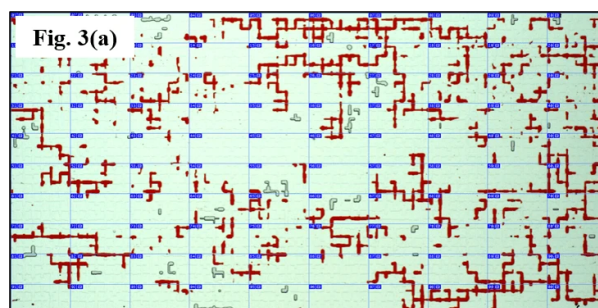
Fig. 1(b)

Wettability Alteration

In order to change the wettability, we diluted aquaphobe-CM solution to different mass fractions using n-hexane to achieve different wettability. We called the solution coating solution. We characterize the wettability of our system by placing a small drop of brine (4% w/v sodium chloride solution) on three treated silicon glass sheets, which have the same material as the microfluidic model. Two of silicon glass sheets were completely submerged in a petri dish filled with coating solutions of different concentrations (5% and 20%). After standing for 24 hours, they were removed and dried. The other one was left untreated. Finally, the wettability of siliceous glass was determined measuring oil, water and surface three-phase contact angles (**Fig. 2**). Contact angles were measured as $20^\circ \pm 2^\circ$ (imbibition), $120^\circ \pm 5^\circ$ (weak drainage) and $160^\circ \pm 5^\circ$ (strong drainage).



In order to verify the contact angle of the pore-throat wall surface of the modified microfluidic model, as shown in **Fig. 3(a)**, the model area (20mm×10mm) was firstly divided into 100 grids (2mm×1mm), and then a solid particle-water-oil phase in each grid was randomly selected with a microscope. The intersection of three phases was the vertex, and the tangents of oil-brine contact surface and solid-water contact surface were used as two sides to determine the three-phase contact angle. Finally, measurement and statistics are carried out and the results are shown as **Fig. 3(b)**, **3(c)** and **3(d)**. The three wettability measurements results are distributed in a nearly normal fashion. When the wettability is imbibition, contact angle is mostly 40° to 60° statistically. There is some difference in the contact angle between the two viscosity ratios at weak and strong drainage, but the contact angle statistics are 110°-125° and 135°-150° respectively, which is in line with the measurement and statistical requirements.



Materials

In our experiments, an aqueous solution of sodium chloride with a mass fraction of 4% was selected as the displaced phase. In addition, we use Ponceau Colors as a dye to make the displaced phase appear red, so that the displaced phase can be clearly distinguished from the displaced phase in the photos or videos captured by the camera. As the viscosity ratio (M) is 1.16, the displaced phase is n-decane, forming a brine-decane fluid displacement system. As to altering the

wettability of the pore-throat wall in the microfluidic model, we chose to dilute aquaphobe-CM solution with hexane as the coating solution to form a hydrophobic film on the wall. The detailed information of each material is shown in **Table 1**.

Table 1

Details of the chemicals used in the study

Chemical	Provider	Commercial name/code	Function
aqueous solution of sodium chloride (4% w/v)	home-made	-	Displacing phase
Decane (98%)	Aladdin	D105231-500ml	Displaced phase
Aquaphobe-CM	Fluorochem	PP1-AQCM	Coating solution
Ponceau Colors	Shanghai Dyestuffs Research Institute Co., Ltd	GB1886.220	Colorant

RESULTS AND DISCUSSION

Oil-Water Two Phase Pore-scale Displacement Pattern

Fig. 4 shows the advancing process of two-phase fluid interface under different wettability and capillary number. In the figure, the color of the invading fluid changes gradually from blue to red in a rainbow pattern, representing the time change of the experiment from the start to the breakthrough. Blue represents the fluid distribution at the moment when the invading fluid just entered in the microfluidic model, and red represents that when the invading phase flows to the breakthrough. In the two-phase displacement experiment, the viscosity ratio (M) of brine to n-decane is 1.16.

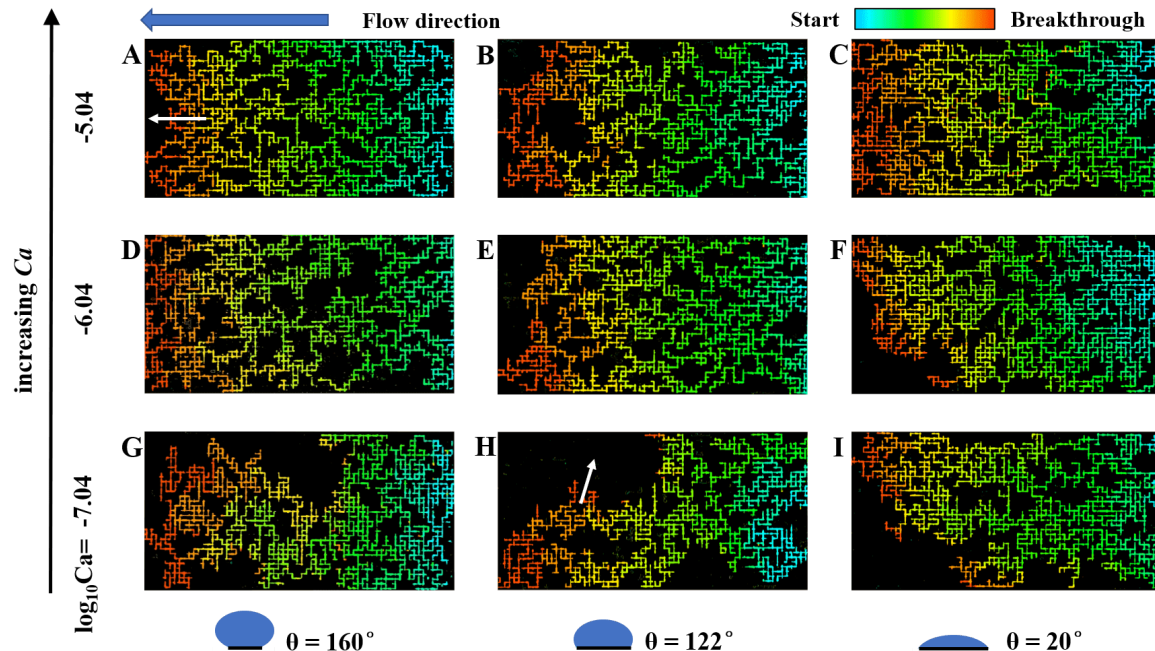


Fig.4 Displacement patterns for different wettability conditions (left to right: $\theta = 160^\circ$, 122° , 20°) and capillary numbers (bottom to top : $Ca = 9.08 \times 10^{-8}$, 9.08×10^{-7} , 9.08×10^{-6}). These patterns correspond to the end of the experiment, which is when the invading fluid reaches the edge of the flow cell. And the viscosity ratios M (viscosity of the displaced fluid divided by the viscosity of the advancing wetting fluid) is fixed at 1.16. All images are oriented in the same way from right to left and the colors from blue to red represent the evolution of the invasion front with time from the beginning to the breakthrough to aid visual comparison.

In the case of brine displacing n-decane (i.e., $M=1.16$), higher flow rate leads to a more stable displacement pattern. In all three wettability cases, smaller flow rate leads to the decrease of capillary number, and the capillary fingering phenomenon is more obvious. As Explained by Lenormand et al., reduced Ca causes displacement to shift from stable to fingering and the result of our experiments are identical with theirs to some extent. Dominated capillary force, the advancing direction of the two-phase fluid interface may be inconsistent with the main flow direction, which may be perpendicular or even opposite to the main flow direction (arrow in **Fig. 4G**). As the capillary force effect gradually weakens, the displacement behavior in any of the above directions will be significantly inhibited. The advancing direction of the interface tends to be the main flow direction (arrow in **Fig. 4A**), and the multiphase seepage tends to be stable. In terms of wettability, it can be found that the displacement patterns are more stable when the pore-throat wall surface is strong drainage or imbibition. **Fig. 4A** and **Fig. 4C** show the two most stable displacement modes in this group of experiments. The phenomenon of capillary fingering during weak drainage is more obvious.

Distribution Features of Two-phase Fluid at Breakthrough

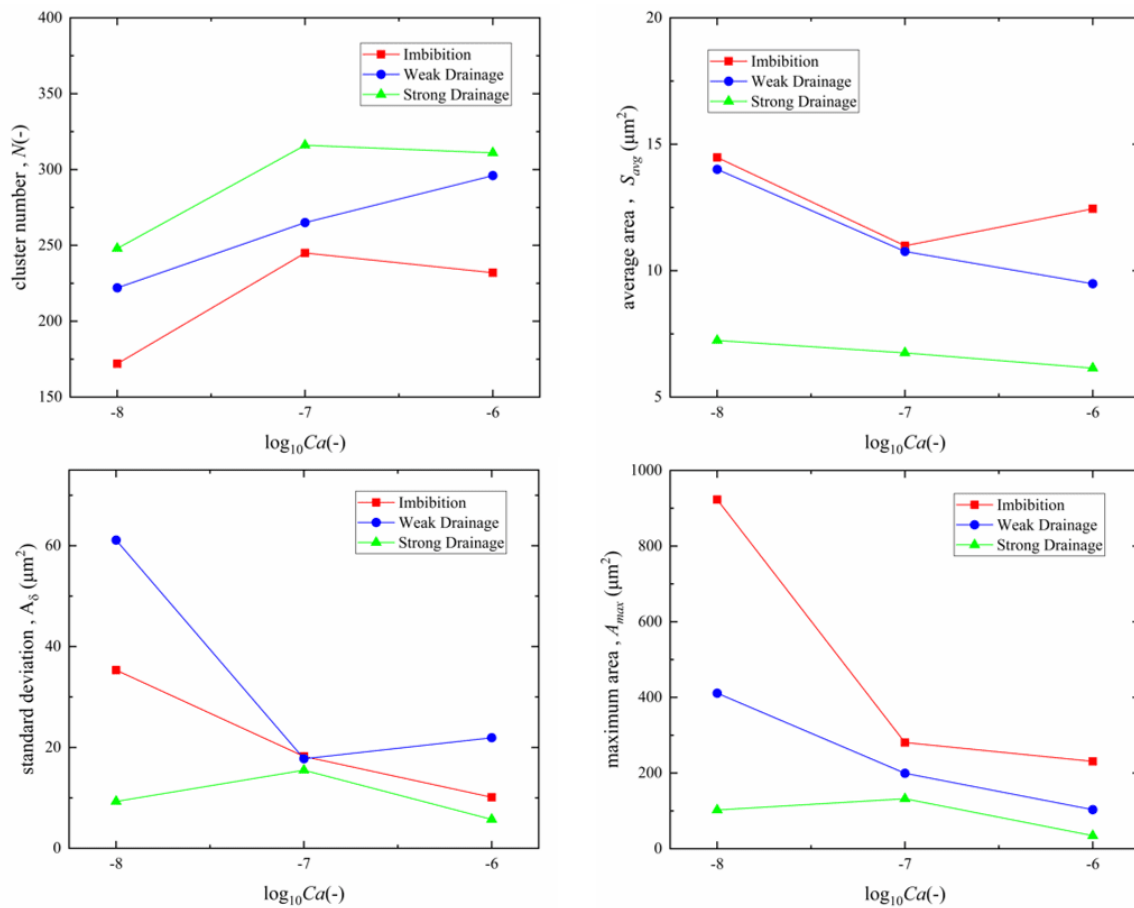


Fig.5 oil cluster morphological statistical parameters for brine-decane displacement (M=1.16)

The binarization diagram of pore-throat and matrix was obtained by extracting the pore of dry the micromodel chip. Then, the remaining oil distribution image of displacement breakthrough was obtained through image processing. The residual oil clusters were counted according to pixel segmentation, and the corresponding morphological statistical parameters were calculated. The statistical parameters include the number of clusters (N), the maximum area of cluster (A_{max}), the average area of cluster (A_{avg}) and the standard deviation of cluster area (A_σ).

In general, there is a positive correlation between the number of oil clusters and contact angle when the viscosity ratio $M=1.16$ (Fig. 5). Under the same wettability condition, the number of oil clusters (N) at medium flow rate and high flow rate is obviously higher than that at low flow rate, and the change rule of A_{max} and A_{avg} is opposite. This may be due to the "fragmentation" of the larger oil clusters as the flow rate increases. Large residue oil clusters are broken by invading phase with high flow rate, resulting in many small clusters, so the number of oil clusters increases, but the average area and maximum area decrease. In the case of small flow rate, the invading phase will choose to flow around the large oil cluster body when encountering each other, so large residue oil clusters will be left at breakthrough.

Influence of Wettability on Displacement Efficiency

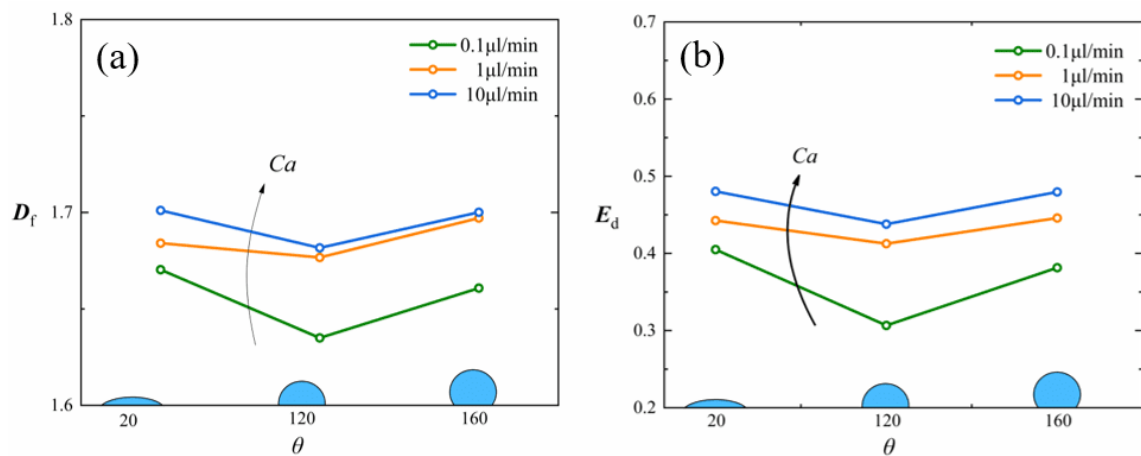


Fig.6 (a) Fractal dimension D_f of the 2D invasion pattern as a function of the static contact angle θ , computed using the box-counting method; (b) Displacement efficiency E_d at different wettability and capillary number.

Displacement efficiency E_d is a function of θ , where E_d is defined as the proportion of oil phase displaced from the microfluidic chip at the end of the experiment, that is, the proportion of invading phase in the micromodel pore.

In the case of $M=1.16$, as shown in **Fig.6** displacement efficiency increases with the increase of capillary number (Ca). At the same viscosity ratio, the displacement efficiency is the lowest at weak drainage ($\phi=120^\circ$). This may be due to the greater heterogeneity of the contact angle under weak drainage, resulting in lower displacement efficiency.

We quantify the invading brine phase complexity by calculating two-dimensional fractal dimension by box counting method. The result positively corresponds to the result of oil displacement efficiency, which can further prove the reliability of the experiment.

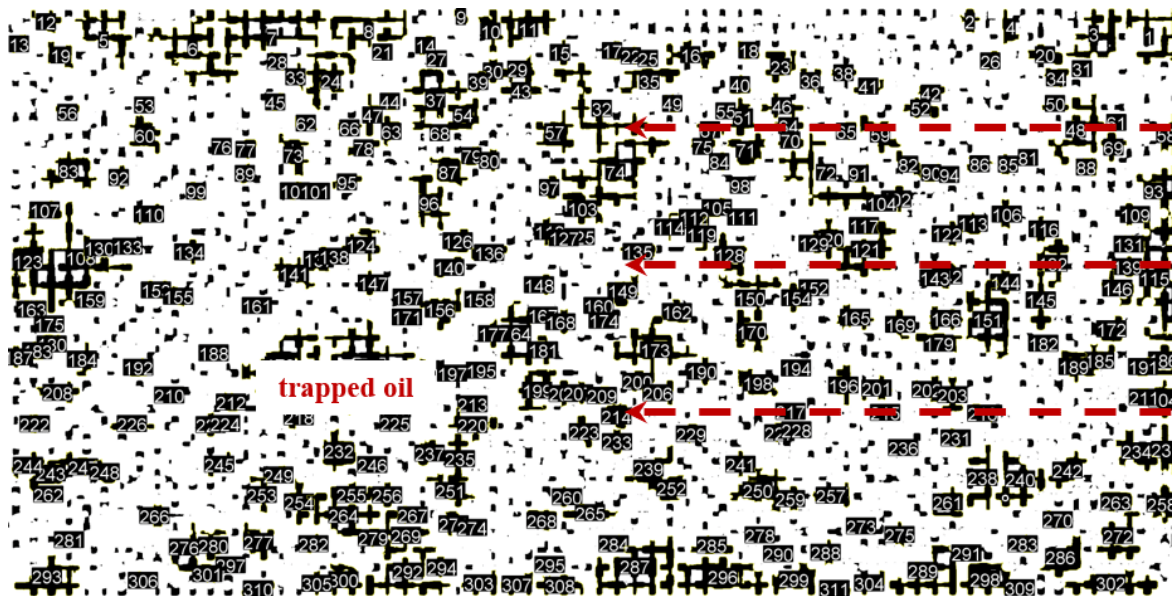


Fig.7 Strong drainage, brine displacing decane and the flow rate is 0.1 $\mu\text{l}/\text{min}$. The numeric marker represents the number of the oil cluster. White is the invading fluid and black is the trapped oil.

Based on the microscopic observation technology in the experimental platform, the distribution of two-phase fluid and the formation process of residual oil clusters at the breakthrough are presented in **Fig. 7**. In the case of brine displacing n-decane, the invading phase streamline is relatively stable, and the flow direction is mostly along the main displacement direction. In addition, the displacement front advance is also uniform. Therefore, the residual oil cluster number and dispersion degree is large, and oil displacement efficiency is high.

Evolution of Injection Pressure

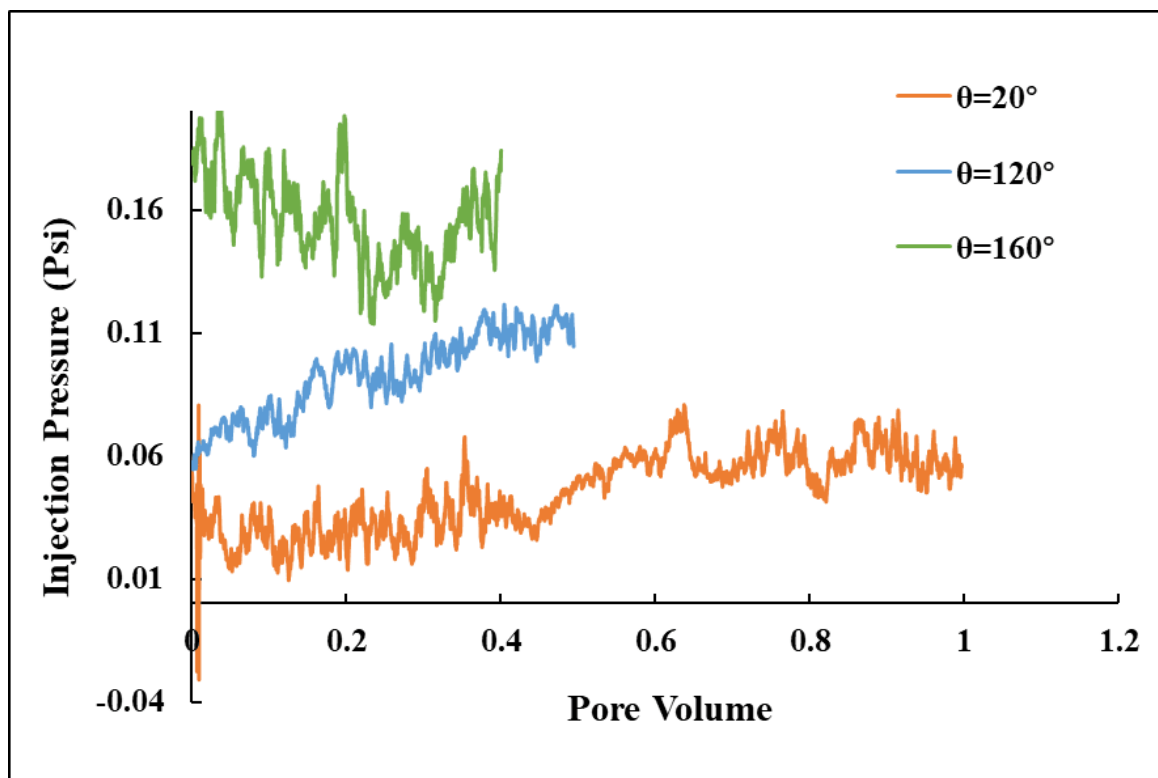


Fig. 8 When brine displacing decane and the flow rate is 0.1 μ l/min, the injection pressure of each wettability changes with PV.

At $M=1.16$ (i.e., brine displacing n-decane), all three wettability at 0.1 μ l/min flow rates varied and stabilized at very low pressures (0-0.2 psi). As shown in **Fig. 8**, the contact angle is positively correlated with the injection pressure. The trend and fluctuation at breakthrough moment is less obvious in this case.

CONCLUSION

- (1) When the displacement pattern is capillary fingering, the high flow rate makes the displacement front more stable and uniform, leading to higher displacement efficiency
 - (2) Just as the experimental results of Lenormand et al., the reduced Ca in our experiment led to the displacement transition from stable to fingering-forward.
 - (3) The displacement patterns of weak drainage are more unstable than strong drainage and imbibition, resulting in lower oil displacement efficiency.
 - (4) In the case of brine flooding decane ($M=1.16$), the high flow rate causes the large residual oil clusters to "break up", resulting in many more small oil clusters.
-

AUTHOR INFORMATION

Nong Kang

Peixing Xu

Shuangmei Zou

Congjiao Xie

REFERENCES

- [1] L.-C. Chang, J.-P. Tsai, H.-Y. Shan *et al.*, “Experimental study on imbibition displacement mechanisms of two-phase fluid using micro model,” *Environmental Earth Sciences*, vol. 59, no. 4, pp. 901-911, 2009.
- [2] D. Rao, M. Girard, and S. Sayegh, “The influence of reservoir wettability on waterflood and miscible flood performance,” *Journal of Canadian Petroleum Technology*, vol. 31, no. 06, 1992.
- [3] X. Zhou, N. R. Morrow, and S. Ma, “Interrelationship of wettability, initial water saturation, aging time, and oil recovery by spontaneous imbibition and waterflooding,” *Spe Journal*, vol. 5, no. 02, pp. 199-207, 2000.
- [4] P. Jadhunandan, and N. R. Morrow, “Effect of wettability on waterflood recovery for crude-oil/brine/rock systems,” *SPE reservoir engineering*, vol. 10, no. 01, pp. 40-46, 1995.
- [5] W. G. Anderson, “Wettability literature survey-part 1: rock/oil/brine interactions and the effects of core handling on wettability,” *Journal of petroleum technology*, vol. 38, no. 10, pp. 1125-1144, 1986.
- [6] B. Zhao, C. W. MacMinn, and R. Juanes, “Wettability control on multiphase flow in patterned microfluidics,” *Proceedings of the National Academy of Sciences*, vol. 113, no. 37, pp. 10251-10256, 2016.
- [7] R. Lenormand, E. Touboul, and C. Zarcone, “Numerical models and experiments on immiscible displacements in porous media,” *Journal of fluid mechanics*, vol. 189, pp. 165-187, 1988.
- [8] M. Sahimi, “Flow phenomena in rocks: from continuum models to fractals, percolation, cellular automata, and simulated annealing,” *Reviews of modern physics*, vol. 65, no. 4, pp. 1393, 1993.
- [9] R. Lenormand, “Liquids in porous media,” *Journal of Physics: Condensed Matter*, vol. 2, no. S, pp. SA79, 1990.
- [10] L. Paterson, “Diffusion-limited aggregation and two-fluid displacements in porous media,” *Physical review letters*, vol. 52, no. 18, pp. 1621, 1984.

